# Mitra: An O-RAN based Real-Time Solution for Coexistence between General and Priority Users in CBRS

Shiva Acharya\*, Shaoran Li\*, Nan Jiang<sup>†</sup>, Yubo Wu\*, Y. Thomas Hou\*, Wenjing Lou\*, Weijun Xie<sup>†</sup>

\* Virginia Tech, Blacksburg, VA, USA

<sup>†</sup> Georgia Institute of Technology, Atlanta, GA, USA

Abstract—To maximize the potential benefit of Citizen Broadband Radio Service (CBRS), efficient coexistence algorithms are urgently needed for the general authorized access (GAA) users. The goal is to allow GAA users to share the same spectrum with priority access license (PAL) users, while providing the required interference protection to PAL users. The main challenge in designing an efficient coexistence solution is the absence of collaboration from the PAL users and the uncertainty in sensed channel information. This paper addresses these problems using a data-driven approach based on limited data samples. We develop a mathematical model based on chance-constrained programming (CCP) to address uncertainty in sensed data samples. By exploiting the idea of the ∞-Wasserstein ambiguity set, we reformulate the CCP problem into a deterministic Mixed-Integer Nonlinear Program (MINLP). We propose an open RAN (O-RAN)-based solution to MINLP at the GAA base station (BS) that delivers a real-time scheduling solution.

### I. INTRODUCTION

To best utilize the precious radio spectrum, the U.S. is taking a lead to explore innovative technologies for spectrum sharing. Most notably, the FCC specified the Citizens Broadband Radio Service (CBRS) band, a 150 MHz band in the 3550-3700 MHz spectrum for sharing among threetier users: the incumbent (DoD), commercial priority access license (PAL) and general authorized access (GAA) users [1]. The incumbent users are predominantly Navy radars along the coast and operate in dynamic protection areas (DPAs). They are strictly protected by the Spectrum Access System (SAS) from interference from PAL and GAA users through channel allocation. In the inland, PAL users should be protected from interference from GAA users, while GAA users do not receive any interference protection and operate on a best-effort basis. As of January 2023, more than 300,000 CBRS BS devices (CBSDs) were deployed in the US [2]. Additionally, there are 500 FCC certified end-user device models that use CBRS [2]. With such rapid growth, efficient coexistence mechanisms are crucial for different-tier users in CBRS.

This paper focuses on the coexistence of the PAL and GAA users on the inland in the CBRS band. Currently, the FCC specifies a PAL protection area (PPA) around a PAL base station (BS). At any point within this PPA, aggregate interference from GAA users cannot exceed  $-80 \, \text{dBm/10MHz}$  [1]. However, it is not clear how this can be achieved in practice. Without an efficient solution to this problem, one would either encounter low spectrum efficiency (e.g., by separating the PAL and GAA BSs sufficiently apart in space or in spectrum), or risk having the PAL users suffer from the GAA users' interference beyond the threshold.

Neither FCC [1] nor WInnForum [3] has offered any solution to achieve efficient coexistence between PAL and GAA users. Recent studies on CBRS (see, e.g., [4], [5]) addressed channel allocation problems to PAL and GAA CB-SDs while protecting incumbent from interference. However, these studies did not address potential interference issues at the user device level during coexistence, i.e., interference from the GAA user devices (not just GAA CBSD) to PAL user devices. In [6] and [7], the authors explored listenbefore-talk (LBT) opportunistic random access techniques for coexistence between GAA and PAL users. Again, they did not consider interference from GAA users to PAL users. Before CBRS, there was much research on the underlay coexistence with the use of cognitive radios (see, e.g., [8]-[11]). But the problems considered in those studies did not exactly address the interference problem in CBRS, which has its specific rules and operating requirements, such as PPA and strict interference threshold, among others [1]. Further, many solutions developed for underlay coexistence either assumed knowledge of the underlying channel distribution (see, e.g., [12], [13]) or assumed perfect channel knowledge (see, e.g., [14], [15]). These solutions are not very useful in practice, as such knowledge is simply unavailable to the GAA CBSD or its users. Some recent work on cognitive radios in underlay has utilized machine learning techniques, such as deep neural networks (DNN) and deep learning (DL) (see, e.g., [16]–[18]). However, none of these works has addressed the uncertainty associated with the interference channel between primary and secondary users.

The goal of this paper is to design a real-time solution for efficient coexistence between GAA and PAL users on the same spectrum. Specifically, we consider the scenario in which a number of GAA users served by a GAA BS are operating in a close neighborhood of PPA. The interference from the GAA users, if not properly controlled, will interfere with the operation of the PAL users. Our objective is to maximize the spectrum efficiency of GAA users while providing interference protection to PAL users with a statistical guarantee. By the "statistical" guarantee, we mean that the probability that the interference from the GAA users to any PAL users exceeds a predefined threshold is strictly kept at a small target value (a.k.a. risk level). The main challenge in this effort is the uncertain nature of channel state information between GAA and PAL users, due to the absence of collaboration between these two tiers of users. Another challenge comes from the fact that for a 5G-compliant GAA service, the scheduling decision (including power control for each GAA user) must

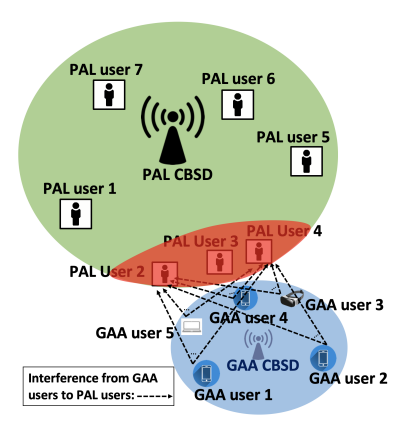


Fig. 1. System Model: GAA users operating in the neighborhood of a PAL's PPA in the same spectrum.

be completed on a 1 ms time scale to meet the requirement of the 5G transmission time interval (TTI).

The main contributions of this paper are:

- We develop a mathematical model to study efficient coexistence between GAA and PAL users in the same spectrum. Instead of assuming partial or full knowledge of channel distributions, our model is purely data driven and only requires a limited number of data samples through sensing, without the cooperation of PAL users.
- To effectively address the inherent uncertainty associated with interference channel, we employ Chance-Constrained Programming (CCP), which offers a strong probabilistic performance guarantee. To address the unknown channel distributions in the chance constraints, we propose to employ ∞-Wasserstein ambiguity set based on the limited number of real-time data samples, which allows us to transform the original CCP problem into a deterministic Mixed Integer Nonlinear Program (MINLP).
- To design a real-time solution, we follow the open RAN (O-RAN) architecture and develop each component of our solution based on different time-scale control loops. Specifically, our proposed solution, codenamed Mitra, includes a non-real-time (non-RT) control loop and a Real-Time (RT) control loop. In Mitra's non-RT control loop, we develop an algorithm to determine the appropriate search radius of the ∞-Wasserstein ambiguity set to ensure that the unknown channel distribution falls within this set with a high probability. In Mitra's RT control loop, we design a real-time algorithm based on the COTS GPU platform.
- Through extensive experiments, we find that Mitra can provide the desired interference protection to PAL users. Furthermore, the running time of Mitra is under 1 ms for all scenarios of practical interest. Mitra is fully compliant with O-RAN architecture and can be readily deployed for O-RAN-based GAA services in CBRS.

## II. SYSTEM MODEL

Consider an outdoor PAL CBSD (base station) operating on a set of licensed contiguous channels (up to 4, each with 10 MHz). For a Category B outdoor CBSD, its maximum transmit power is 47 dBm/10MHz. Based on the ITU outdoor path loss model, for CBSD's signal strength to decay to -96 dBm/10MHz, the radius is about 2.5 km (see Fig. 1). The FCC has established a PPA against interference from nearby GAA users. In our system model, we assume that the PPA aligns with the corresponding PAL's CBSD coverage area (within a radius of 2.5 km from a PAL's CBSD). At any point inside the PPA, the FCC rule [1] requires that aggregate cochannel interference from nearby GAA users does not exceed a threshold of -80 dBm/10MHz. Within the PPA, we assume that there is a set of PAL users, each with a peak transmit power of 23 dBm/10MHz [3].

Consider an indoor<sup>1</sup> Category A GAA CBSD that operates outside of the PPA, with a non-overlapping coverage area. The maximum transmission power of the GAA CBSD is 30 dBm/10MHz. Based on the ITU indoor path loss model, we assume that the transmission range of GAA CBSD is around 80 meters. The maximum transmission power of the GAA user devices is 23 dBm/10MHz [3].

The nonoverlapping coverage areas of the PAL and GAA CBSDs will guarantee that the two BSs do not interfere with each other. However, the transmission by the GAA users in the GAA CBSD coverage area can still cause interference to PAL users in the PAL CBSD coverage area, particularly those that are close to the border of the GAA's operating area (see Fig. 1). Therefore, our goal is to ensure that *aggregate* interference from GAA users does not exceed the interference threshold of -80 dBm/10MHz for these PAL users.

To investigate this problem, we consider downlink data transmission on the PAL side and uplink data transmission on the GAA side (see Fig. 1), i.e. the scenario where PAL users may be potentially interfered with by GAA users.<sup>2</sup> To ensure that aggregate interference from GAA users to nearby PAL users is below the threshold, power control is needed for GAA users. However, power control requires channel information between GAA and PAL users. But due to the absence of collaboration between GAA and PAL users, an indirect mechanism is needed to estimate such channel conditions.

We assume that a GAA user estimates the channel conditions to its nearby PAL users by overhearing the known Sounding Reference Signals (SRS) during their uplink transmissions. On the basis of channel reciprocity in the TDD mode, a GAA user can estimate the channels between itself and its nearby PAL users. However, due to physical impairments, environmental conditions, and estimation errors, there is much *uncertainty* involved in making an accurate estimate

<sup>&</sup>lt;sup>1</sup>The analysis for the case for an outdoor Category B GAA CBSD follows the same token.

<sup>&</sup>lt;sup>2</sup>The case where the GAA users may be interfered, i.e., uplink transmission at the PAL user side and downlink transmission at the GAA user side, is not an issue as the GAA users are not offered any interference protection from the PAL users per FCC [1].

of channel gains between a GAA user and its neighboring PAL users. To address such uncertainty in channel estimation, we employ *Chance-Constrained Programming* (CCP). The goal is to ensure that the interference from GAA users to PAL users does not exceed the PAL interference threshold with high probability (e.g., 99%).

## III. PROBLEM FORMULATION

## A. Mathematical Model

We employ TDD for the uplink and downlink data transmission at the GAA CBSD. Based on 5G terminology, frequency and time resources are classified as sub-carriers and TTI, respectively. Twelve contiguous subcarriers in one TTI are referred to as a resource block (RB). According to 5G standards [19], contiguous RBs can be grouped together to form an RB group (RBG) for allocation of RBs. In this paper, we adopt this RBG concept for resource allocation. We employ the single-user OFDMA technique for data transmission, where each RBG can be assigned to at most one user.

Let  $\mathcal{M}$  represent a set of PAL users, i.e.,  $\mathcal{M}=\{1,2,\cdots,j,\cdots,M\}$ . Let  $\mathcal{N}$  represent a set of GAA users, i.e.,  $\mathcal{N}=\{1,2,\cdots,i,\cdots,N\}$ , and let  $\mathcal{G}$  represent a set of RBGs, i.e.,  $\mathcal{G}=\{1,2,\cdots,g,\cdots,G\}$ . Denote  $x_i^g(t)$  as a binary variable to represent whether or not GAA user i is assigned to an RBG g in TTI t, i.e.,

$$x_i^g(t) = \begin{cases} 1 & \text{if GAA user } i \text{ transmits to its BS on RBG } g, \\ 0 & \text{otherwise.} \end{cases}$$

Based on the single-user OFDMA assumption, each RBG g can be assigned to at most one user. We have:

$$\sum_{i \in \mathcal{N}} x_i^g(t) \le 1 \quad (g \in \mathcal{G}) . \tag{1}$$

Denote  $p_i^g(t)$  as the transmission power of GAA user i on RBG g in TTI t and  $P_i^{\max}$  as the maximum power limit, respectively. If  $x_i^g(t)=1$ , then we must have  $0< p_i^g(t) \leq P_i^{\max}$ ; otherwise,  $p_i^g(t)=0$ . Combining the two cases, we have:

$$0 \le p_i^g(t) \le x_i^g(t) P_i^{\max} \quad (i \in \mathcal{N}, g \in \mathcal{G}) . \tag{2}$$

Furthermore, the total transmit power allocated to a GAA user across all RBGs must not exceed the maximum power limit. That is,

$$\sum_{g \in \mathcal{G}} p_i^g(t) \le P_i^{\max} \quad (i \in \mathcal{N}) . \tag{3}$$

Denote  $h_{ij}^g(t)$  as the channel gain between GAA user i and PAL user j on RBG g in TTI t. Due to the many uncertainties in estimating  $h_{ij}^g(t)$ , one cannot assume any knowledge of its distribution. Our goal is to ensure that the aggregate interference from the GAA users to each PAL user is upper bounded by the interference threshold set by FCC (denoted as I) with a high probability  $(1-\epsilon)$ , where  $\epsilon$  is a small number and is called a *risk parameter*. We have:

$$\mathbb{P}\left\{\sum_{i\in\mathcal{N}}\sum_{g\in\mathcal{G}}h_{ij}^g(t)p_i^g(t)\leq I\right\}\geq 1-\epsilon\quad (j\in\mathcal{M})\ . \tag{4}$$

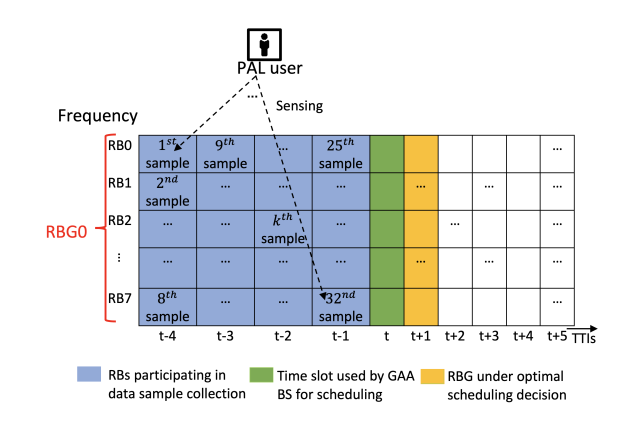


Fig. 2. An illustration of TTI-based transmission pattern at a GAA user. Sensing (overhearing of interference channel) occurs in the blue TTIs while computation of scheduling decision occurs during the green TTI, which will be applied in the yellow TTI.

To represent the double sum in  $\mathbb{P}\{\cdot\}$  in a more compact form, denote  $\mathbf{h}_i(t)$  as a row vector as follows:

$$\mathbf{h}_{j}(t) = \left[ h_{1j}^{1}(t), \cdots, h_{1j}^{G}(t), \cdots, h_{Nj}^{1}(t), \cdots, h_{Nj}^{G}(t) \right] . (5)$$

Denote  $\mathbf{p}(t)$  as a column vector as follows:

$$\mathbf{p}(t) = [p_1^1(t), \dots, p_1^G(t), \dots, p_N^1(t), \dots, p_N^G(t)]^T .$$
 (6)

Then, constraint (4) can be written as:

$$\mathbb{P}\left\{\mathbf{h}_{i}(t)\mathbf{p}(t) \leq I\right\} \geq 1 - \epsilon \quad (j \in \mathcal{M}). \tag{7}$$

Since we do not assume any knowledge of  $\mathbf{h}_i(t)$ , we rely on a sensing (measurement)-based technique to estimate its distribution. For example, SDR-based sensing techniques are commonly employed to analyze the performance of LTE networks by sniffing downlink control information [20]. A similar SDR-based technique can be employed to sense the gain of the interference channel in real time here. Given that each RB occupies a narrow band and that the duration of a TTI is short (1 ms or shorter), the channel behavior within the same RBG over a few contiguous TTIs should follow the same distribution. As shown in Fig. 2, we can use this group of K (blue) RBs (32 in the figure) to sense the interference channel (through the SRS signals of PAL users) and collect K data samples. Note that only a portion of symbols in these (blue) RBs are used for sensing (overhearing), while the others are used for uplink transmission to the GAA BS. At TTI t, the GAA BS will use these inputs to calculate the RBG allocation and its power levels for TTI (t+1).

Denote  $\hat{\mathbf{h}}_{j}^{k}(t)$  as the k-th i.i.d. sample vector  $(k = 1, 2, \cdots, K)$  w.r.t  $\mathbf{h}_{j}(t)$  that will be used at the GAA BS in TTI t. Denote  $\hat{\mathbf{h}}_{j}(t)$  as the row vector that represents the channel gain vector solely based on the K i.i.d. samples. Then we can represent the probability mass function for  $\hat{\mathbf{h}}_{j}(t)$  as follows:

$$\mathbb{P}\left\{\hat{\mathbf{h}}_{j}(t) = \hat{\mathbf{h}}_{j}^{k}(t)\right\} = \frac{1}{K}.$$
 (8)

In Section III-C, we will use  $\infty$ -Wasserstein ambiguity set to connect this empirical distribution to the unknown distribution.

#### B. Problem Formulation

For the objective function, we consider *proportional fair* (PF) throughput across all GAA users for their uplink transmission. The idea is that even under power control (so that the interference threshold at the PAL users is satisfied through chance constraints), we still want to maximize the total throughput utility in the GAA network. Denote  $h_{iB}^g(t)$  as the channel gain between GAA user i and the GAA BS on RBG g. Denote  $r_i^g(t)$  as the (bandwidth) normalized capacity of GAA user i on RBG g at TTI t, i.e.,

$$r_i^g(t) = \log_2 \left( 1 + \frac{h_{iB}^g(t)p_i^g(t)}{PL_{\rm PAL}(d_{\rm PAL}) \cdot P_{\rm PAL} + \sigma^2} \right) \; , \label{eq:right}$$

where  $P_{\rm PAL}$  represents the transmission power of PAL BS,  $\sigma^2$  denotes the thermal noise at the GAA CBSD on each RBG g, and  $PL_{\rm PAL}(d_{\rm PAL})$  represents the path loss between the PAL BS and GAA BS. Then the PF throughput objective is given by:

$$\sum_{i \in \mathcal{N}} \sum_{g \in \mathcal{G}} \frac{r_i^g(t)}{\tilde{R}_i(t-1)} , \qquad (9)$$

where  $\tilde{R}_i(t-1)$  is an input parameter that represents the exponentially smoothed average data rate of user i up to TTI (t-1) over a window size of w TTIs.  $\tilde{R}_i(t-1)$  is a constant value at TTI t and can be calculated as follows:

$$\tilde{R}_i(t-1) = \frac{w-1}{w}\tilde{R}_i(t-2) + \frac{1}{w}R_i(t-1).$$
 (10)

In (10),  $R_i(t-1)$  represents the total data rate of user i at TTI (t-1) over all its scheduled RBGs, which is computed at the BS based on the scheduling results from TTI (t-2). For the window size (w) in the above expression, a typical value of 100 TTIs is considered. Furthermore,  $\tilde{R}_i(t-2)$  is a constant value available to the GAA BS at TTI (t-1).

In this paper, we are interested in maximizing the PF throughput of all GAA users while ensuring their aggregate interference to each PAL user below a threshold with high probability. At TTI t, this problem can be formulated as:

(OPT) 
$$\max \sum_{i \in \mathcal{N}} \sum_{g \in \mathcal{G}} \frac{r_i^g(t)}{\tilde{R}_i(t-1)}$$

s.t. RB allocation constraints (1), GAA users' power constraints (2) and (3), PAL interference threshold guarantee (7), Empirical channel distribution of  $\mathbf{h}_j(t)$  (8), variables:  $x_i^g(t) \in \{0,1\}, \quad p_i^g(t) \geq 0$ .

### C. A Reformulation

The major difficulty with OPT lies in chance constraints (7), due to the unknown distribution of the interference channel gain  $\mathbf{h}_j$ . Denote the unknown distribution of  $\mathbf{h}_j$  as  $\mathbb{P}_{\mathbf{h}_j}$ .

We will use  $\infty$ -Wasserstein distance to connect the unknown distribution  $\mathbb{P}_{\mathbf{h}_j}$  and the empirical distribution  $\mathbb{P}_{\hat{\mathbf{h}}_i}$  in (8).

Define  $W_{\infty}(\mathbb{P}_{\zeta_1}, \mathbb{P}_{\zeta_2})$  as the  $\infty$ -Wasserstein distance between two marginal distributions  $\mathbb{P}_{\zeta_1}$  and  $\mathbb{P}_{\zeta_2}$  equipped with  $L_2$  norm. Denote  $\mathcal{F}_{W_{\infty}}(\theta_j)$  as the  $\infty$ -Wasserstein ambiguity set, which is a family of probability distributions such that the  $\infty$ -Wasserstein distance from the empirical distribution  $\mathbb{P}_{\hat{\mathbf{h}}_j}$  to the unknown distribution  $\mathbb{P}_{\mathbf{h}_j}$  is bounded by a constant (radius)  $\theta_j$ , i.e.,

$$\mathcal{F}_{W_{\infty}}\left(\theta_{j}\right) = \left\{\mathbb{P}_{\mathbf{h}_{j}}: W_{\infty}\left(\mathbb{P}_{\mathbf{h}_{j}}, \mathbb{P}_{\hat{\mathbf{h}}_{j}}\right) \leq \theta_{j}, \quad \mathbf{h}_{j} \in \mathbb{R}_{+}^{1 \times NG}\right\} ,$$

for  $j \in \mathcal{M}$ , where  $\mathbb{R}_+^{1 \times NG}$  is the positive real space for a  $1 \times NG$  row vector. The larger the number of data samples, the closer our empirical distribution is to the true distribution.

Since we plan to use only limited sensing data samples to achieve performance guarantees to the PAL users, we can instead adjust the radius value  $\theta_j$  so that the unknown distribution lies in the  $\infty$ -Wasserstein ambiguity set, with a high probability. However, the larger the  $\theta_j$ , the more (worst-case) probability distributions we need to consider in the Wasserstein ball, which will degrade our objective value. So it is important that we find an appropriate value for  $\theta_j$  such that

$$\mathbb{P}_{\mathbf{h}_{i}} \in \mathcal{F}_{W_{\infty}}(\theta_{i}) \quad (j \in \mathcal{M}) \tag{11}$$

holds almost surely. We will show how to determine  $\theta_j$  in Section IV-A.

To ensure (7) hold, it is sufficient to have

$$\inf_{\mathbb{P}_{\mathbf{d}_j} \in \mathcal{F}_{W_{\infty}}(\theta_j)} \mathbb{P} \left\{ \mathbf{d}_j \mathbf{p} - I \le 0 \right\} \ge 1 - \epsilon \quad (j \in \mathcal{M}) , \quad (12)$$

where  $\mathbb{P}_{\mathbf{d}_j}$  represents a distribution inside  $\mathcal{F}_{W_{\infty}}(\theta_j)$ . Based on [21], it can be shown that (12) can be reformulated as follows:

$$\mathbb{P}_{\hat{\mathbf{h}}_j} \left\{ \hat{\mathbf{h}}_j \mathbf{p} - I + \theta_j \| \mathbf{p} \|_2 \le 0 \right\} \ge 1 - \epsilon \quad (j \in \mathcal{M}) , \quad (13)$$

which is based on the empirical distribution  $\mathbb{P}_{\hat{\mathbf{h}}_i}$ .

But for the empirical distribution  $\mathbb{P}_{\hat{\mathbf{h}}_j}$ , we only have K sensing data samples at the GAA users. So among these K samples, there should be at least  $\lceil K \cdot (1-\epsilon) \rceil$  instances that the inequalities  $(\geq)$  should hold. To model this requirement, we define an indicator function  $\mathbb{I}\{\cdot\}$ , which is 1 when the argument holds and 0 otherwise. We have, for  $j \in \mathcal{M}$  and  $k \in K$ 

$$\sum_{k \in \mathcal{K}} \mathbb{I}\left\{\hat{\mathbf{h}}_{j}^{k} \mathbf{p} - I + \theta_{j} \|\mathbf{p}\|_{2} \le 0\right\} \ge K \cdot (1 - \epsilon) . \tag{14}$$

Now we can replace (7) in OPT with (14). Also, with the inclusion of (14), (8) in OPT is no longer needed. We have:

(OPT-R) 
$$\max \sum_{i \in \mathcal{N}} \sum_{g \in \mathcal{G}} \frac{r_i^g}{\tilde{R}_i(t-1)}$$

s.t. RB allocation constraint (1), GAA users' power constraint (2) and (3), PAL interference threshold guarantee (14), variables:  $x_i^g \in \{0,1\}, \quad p_i^g \geq 0.$ 

<sup>&</sup>lt;sup>3</sup>The potential uncertainty in  $h_{iB}^g(t)$ 's is less of a concern than  $h_{ij}^g(t)$ 's as it will not violate any interference protection (statistical performance guarantee) on the PAL users. So we will not employ chance constraints on the  $h_{iB}^g(t)$ 's, as doing so will unnecessarily complicate the problem.

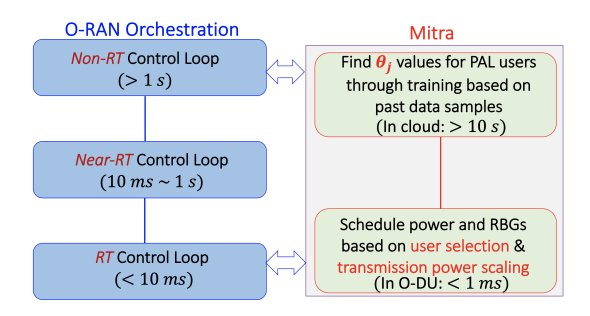


Fig. 3. Mitra: An overview in the O-RAN architecture

Note that in OPT-R, we are no longer dealing with the unknown distribution  $\mathbb{P}_{\mathbf{h}_j}$ , but rather, we are only using the K data samples (in (14)).

For OPT-R, although  $r_i^g$  in the objective function involves a logarithmic function, it does not pose much difficulty since it can be approximated by a convex hull relaxation [22]. The main challenge is the indicator function in (14). One technique to address this problem is through a bi-level formulation, which allows to transform our problem into an upper-level problem and a lower-level problem. The upper-level problem is to check the feasibility of the solutions obtained from the lower-level problem, while the lower-level problem can be solved by a convex approximation technique called ALSO-X [21]. However, this approach, as we shall compare in Section V, incurs excessively high computation time even for small-size networks. To meet the 1 ms real-time requirement, a new solution is needed.

## IV. MITRA: A DESIGN OVERVIEW

We present a real-time solution to OPT-R, codenamed *Mitra*. <sup>4</sup> Mitra can offer a high-performing feasible solution (including providing interference protection to the PAL users) with a computation time under 1 ms (consistent to 5G NR numerology 0 [23]). Mitra conforms to the latest O-RAN architecture [24] and consists of two components: a non-RT component and a RT component, corresponding to the non-RT and RT control loops in O-RAN, respectively. <sup>5</sup> The Mitra algorithm runs at the GAA BS. Below we present the design details of the non-RT and RT control loops in Mitra.

# A. Non-RT Control Loop

As shown in Fig. 3, in the non-RT control loop, we need to determine an *appropriate* value of  $\theta_j$  for all PAL users. If  $\theta_j$ 's are set too large, the radius of the corresponding Wasserstein ball will also be too large, leading to excessively large search space for the OPT-R problem. On the other hand, if  $\theta_j$ 's are set too small, the radius of the Wasserstein ball will also be small, leading to an infeasible solution to OPT-R with a high probability.

We propose to determine  $\theta_j$ 's by employing *cross-validation* and *bisection search* based on a large set of previous data samples of interference channel gain. Intuitively, the  $\theta_j$ 's

are directly proportional to their Bessel corrected standard deviations in their data samples. That is, the higher the standard deviation, the larger the variation and search space, and thus the larger the corresponding value of  $\theta_j$  should be set. Therefore, it is reasonable to use this information to determine the *relative* sizes among the  $\theta_j$ 's. Specifically, we let

$$\begin{bmatrix} \theta_{1} \\ \vdots \\ \theta_{M} \end{bmatrix} = \rho \cdot \begin{bmatrix} \sqrt{\frac{1}{K-1} \sum_{k=1}^{K} \left( \left\| \hat{\mathbf{h}}_{1}^{k} - \frac{\sum_{k=1}^{K} \hat{\mathbf{h}}_{1}^{k}}{K} \right\|_{2}^{2} \right)} \\ \vdots \\ \sqrt{\frac{1}{K-1} \sum_{k=1}^{K} \left( \left\| \hat{\mathbf{h}}_{M}^{k} - \frac{\sum_{k=1}^{K} \hat{\mathbf{h}}_{M}^{k}}{K} \right\|_{2}^{2} \right)} \end{bmatrix},$$
(15)

where each  $\theta_j$  is directly proportional to its standard deviation through a common scaling factor  $\rho$  and a set of K data samples is used.

For cross-validation, we divide past data samples into two sets  $\mathcal{U}_1$  and  $\mathcal{U}_2$ , each consisting of a number of windows (each window consisting of K data samples).  $\mathcal{U}_1$  is used to find a starting point for  $\theta_j$  based on the relationship with the Bessel corrected standard deviation mentioned above.  $\mathcal{U}_2$  is used to solve OPT-R and obtain power allocation results  $(p_i^g)$ . Then for each PAL user  $j \in \mathcal{M}$ , we compare the actual interference  $(\mathbf{h}_j \mathbf{p})$  with its threshold I and count the number of violations from V channel instances  $(\mathbf{h}_j)$  to compute the actual probability of violation  $(\epsilon_j^*)$ . To improve the precision of our cross-validation, we compute the average of the actual probability of violation for each PAL user on all windows of  $\mathcal{U}_2$ .

For bisection search, we tune a scaling factor  $\rho$  for all  $\theta_i$ 's proportionally based on their relative relationship through the Bessel-corrected standard deviation. First, we set the initial upper and lower bounds for this unknown scaling factor to be sufficiently large and small numbers, respectively. In each iteration, we set the current (new) scaling factor as the midpoint of the current upper and lower bound values. We compare the averaged actual violation probability of each PAL user  $(\bar{\epsilon_i}^*)$  with the target risk level  $\epsilon$  and update their flag to be 1 if  $\bar{\epsilon_i}^*$  is greater than  $\epsilon$ . Then, based on the sum of all the flags assigned to each PAL user, we increase the lower bound value to the current scaling factor if the total flag count is greater than 0, or decrease the upper bound value to the current scaling factor if otherwise. We terminate the iteration if the normalized gap between the upper and lower bound values is below a small target value.

Once we find new  $\theta_j^*$  values, we pass them to Mitra's RT control loop. The period to update  $\theta_j^*$  values is on the order of tens of seconds and is typically performed in the cloud per O-RAN specification [24].

## B. RT Control Loop

To minimize computation time, we employ the GPU and exploit parallel computing as much as possible. The pseudocode

<sup>&</sup>lt;sup>4</sup>Mitra is a Hindu god known as a protector of treaties and friendship.

<sup>&</sup>lt;sup>5</sup>In O-RAN, there is also a near-RT control loop that sits between non-RT and RT control loops. This near-RT control loop is not needed in Mitra.

## Algorithm 1 RT component in Mitra

```
    input: ĥ<sub>j</sub><sup>k</sup>, h<sub>iB</sub><sup>g</sup>, R̂<sub>i</sub>(t - 2), R<sub>i</sub>(t - 1), w, θ<sub>j</sub>*, I, ε
    output: p<sub>i</sub><sup>g</sup>, x<sub>i</sub><sup>g</sup>
    Compute R̂<sub>i</sub>(t - 1) using (10)
    Reduce search space based on priority metric and obtain S sub-problems
    parfor S sub-problems do
    Generate an initial solution using (17)
    Adjust transmission power per Algorithm 2
    Compute achieved objective value
    end parfor
    Select the solution with the largest objective value as the final solution
```

for the RT control loop is given in Algorithm 1.

**Reducing Search Space:** To best utilize the COTS GPU parallel computing platform, we first divide our problem (OPT-R) into independent subproblems that can be solved in parallel. Based on the RBG allocation constraint (1) in OPT-R, we can first reduce the search space for a given RBG by reducing the set of eligible GAA users (line 4 in Algorithm 1).

To differentiate GAA users in terms of eligibility, we introduce a *priority metric*,  $\eta_i^g$ , if GAA i is assigned to RBG g. Specifically, we define

$$\eta_i^g = \frac{h_{iB}^g}{\tilde{R}_i(t-1)} \quad (i \in \mathcal{N}, g \in \mathcal{G}). \tag{16}$$

This definition is motivated by the fact that the better the channel  $(h_{iB}^g)$ , the higher the priority. On the other hand, the lower the long-term average data rate up to (t-1) TTI  $(\tilde{R}_i(t-1))$  is, the higher the priority metric  $h_{iB}^g$  should be, since our objective function in OPT-R is PF.  $R_i(t-1)$  is calculated using (10) based on the value of  $\tilde{R}_i(t-2)$ ,  $R_i(t-1)$ , and the size of sliding window w (line 3 in Algorithm 1).

Based on this priority metric, for each RBG g, we can sort  $\eta_i^g$  for  $i=1,2,\cdots,N$  and select L users (out of N) with the highest priority metric values for further consideration. Since each RBG g can be assigned to L GAA users, we have a total of  $L^G$  possible assignments. Suppose that our GPU hardware can handle only S subproblems in parallel; we will have to choose S subproblems from the total of  $L^G$  subproblems.

We propose to employ random sampling, by assigning a probability for each GAA user (among L) w.r.t. a given RBG g. This probability can be directly proportional to the priority metric  $\eta_i^g$  or uniform. Given the large number of S, the final result will not be very sensitive to the settings of these probabilities, as long as each GAA user in the set L has a reasonable probability of being chosen.

**Initializing Transmission Power in Each Solution:** For each sub-problem (from a total of S sub-problems), we will determine transmission power for GAA user i on each RBG g ( $p_i^g$ ). Once they are determined,  $x_i^g$ 's can also be easily determined (since  $x_i^g = 1$  if  $p_i^g > 0$  and  $x_i^g = 0$  otherwise).

# Algorithm 2 Tuning Transmission Power

```
1: input: \hat{\mathbf{h}}_{j}^{k}, p_{i}^{g} (initial), \theta_{j}^{*}, \epsilon, I
2: output: p_{i}^{g} for all i \in \mathcal{N}, g \in \mathcal{G}
      parfor j \in \mathcal{M} do
 4:
             for k \in \mathcal{K} do
                    Calculate \hat{\mathbf{h}}_{i}^{k}\mathbf{p}+\theta_{i}^{*}\left\Vert \mathbf{p}\right\Vert _{2}
  5:
  6:
  7:
             Sort the K interference values for PAL user j from
       lines 4-6 in ascending order
             Set c_i as the value of the [K \cdot (1 - \epsilon)]-th element in
       the above sorted set for PAL user j
             Calculate individual scaling factor \delta_j := \frac{1}{C_i}
10:
      end parfor
      Set common scaling factor \alpha := \min_{j \in \mathcal{M}} \delta_j
11:
       parfor i \in \mathcal{N} do
             parfor g \in \mathcal{G} do
13:
                    Set p_i^g := \alpha \cdot p_i^g
14:
             end parfor
15:
16: end parfor
17: parfor i \in \mathcal{N} do
             if \sum p_i^g > P_i^{max} then
18:
                   \begin{array}{c} \mathbf{perfor} \ \mathbf{parfor} \ g \in \mathcal{G} \ \mathbf{do} \\ \mathrm{Set} \ p_i^g := p_i^g \cdot \frac{P_i^{\mathrm{max}}}{\sum p_i^g} \end{array}
19:
20:
                    end parfor
21:
22:
             end if
23: end parfor
```

As a start, we initialize  $p_i^g$  as follows:

$$p_i^g = \frac{P_i^{max}}{G} \cdot u_i^g \,, \tag{17}$$

where  $P_i^{max}$  is the maximum transmission power limit of GAA user i over all RBGs G and  $u_i^g$  is a random number drawn from a uniform distribution, i.e.,  $u_i^g \in U(0,1]$ . Although  $p_i^g$ 's are randomly generated, they will be further tuned in Algorithm 2.

Adjusting Transmission Power in Each Solution: To ensure the feasibility of interference constraint (14) and maximum transmission power constraint (3) are satisfied, we need to tune the initial transmission power  $(p_i^g)$ . We propose Algorithm 2 to perform these two tasks.

For (14), we have K indicator functions associated with each PAL user  $j \in \mathcal{M}$ . We must ensure at least  $\lceil K \cdot (1-\epsilon) \rceil$  indicator functions are satisfied for each PAL user. Based on (14), we first calculate  $\hat{\mathbf{h}}_j^k \mathbf{p} + \theta_j^* \|\mathbf{p}\|_2$  for each PAL user j for  $k=1,2,\cdots,K$  (lines 4–6 of Algorithm 2). Next, we sort these K values in ascending order for each PAL user j by employing parallel sorting (line 7). Denote  $c_j$  as the value of the  $\lceil K \cdot (1-\epsilon) \rceil$ -th element in this sorted set for the PAL user j. Then we can find the value of  $c_j$  for each of the PAL users (line 8). Subsequently, we can find an individual scaling factor  $\delta_j$  based on  $c_j$  to ensure that at least  $\lceil K \cdot (1-\epsilon) \rceil$  indicator

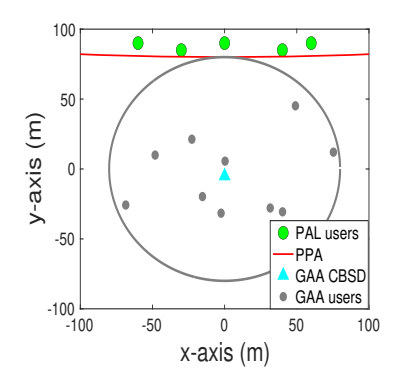


Fig. 4. A network topology with 5 PAL users and 10 GAA users.

functions in (14) are satisfied for the PAL user j (line 9). Since  $\delta_j$ 's differ among the PAL users, we can find a common scaling factor  $\alpha$  for all the PAL users by taking the minimum of  $\delta_j$ 's (line 11). Based on this common scaling factor  $\alpha$ , we can scale the initial transmission power by this factor (lines 12–16). At this point, the probabilistic interference guarantee constraint (14) for all PAL users is satisfied.

To ensure that the transmission power limit constraint (3) is met, we need to check whether, for each GAA user  $i \in \mathcal{N}$ , its total transmission power on all RBGs  $(\sum_{g \in \mathcal{G}} p_i^g)$  is greater than its maximum power limit  $P_i^{max}$  (line 18). If yes, then we need to scale down by  $P_i^{\max}/\sum_{g \in \mathcal{G}} p_i^g$  over all its RBGs (line 20).

Once all  $p_i^g$ 's are determined, we can easily determine the corresponding  $x_i^g$  (that is,  $x_i^g = 1$  if  $p_i^g > 0$  and 0 otherwise). It is easy to show that this solution is feasible for OPT.

Finding the final solution: Now for each of the S feasible solutions, we compute its objective value achieved based on  $p_i^g$ 's and  $x_i^g$ 's. This step is done in parallel for all the S subproblems. Then we select the solution with the best objective value as our final solution. Algorithm 1 summarizes the RT control loop.

### V. PERFORMANCE EVALUATION

In this section, we evaluate the performance of Mitra. For the non-RT control loop, we implement it in MATLAB version R2018b on a 16-core Intel Xeon E5-2687w CPU. For the RT control loop, we implement it on NVIDIA Tesla V100 GPU (with 5120 CUDA cores) with CUDA 12.0 Toolkit [25].

### A. Parameter Settings

The network topology used in our performance evaluation is shown in Fig. 4, which follows the system model in Fig. 1. Not shown in Fig. 4 is the PAL BS (Cat. B CBSD), with a transmission power of 47 dBm. We employ the ITU outdoor path loss model [26] for the PAL BS as follows:  $PL_{\rm PAL}(d_{\rm PAL}) = 128.1 + 37.6 \times \log_{10}(d_{\rm PAL})$  (in dB), where  $d_{\rm PAL}$  represents the distance away from the PAL BS (in km). We assume that the transmission range of the PAL BS is 2.5 km.

The GAA BS (Cat. A CBSD) is shown at the origin of Fig. 4 and lies outside the transmission range of the PAL BS. It has a transmission power of 25 dBm. We use the ITU indoor path loss model [26] for the GAA BS as follows:  $PL_{\rm GAA}(d) = 38 + 30 \times \log_{10}{(d)}$  (in dB), where d is the distance away from a GAA BS (in meters). We assume that the transmission range of the GAA BS is 80 m. The distance between the PAL BS and the GAA BS is set to 2.58 km.

We consider 5 PAL users near the GAA BS's radius and 10 GAA users within the transmission radius of the GAA BS (see Fig. 4). The coordinates of the PAL users indexed 1 to 5 are (-60, 90), (60, 90), (40, 85), (-30, 85), (0, 90), respectively, all in meters. The coordinates of the GAA users indexed 1 to 10 are randomly generated based on a normal distribution. They are (75.3664, 12.0139), (0.3124, 5.5873), (-2.4602, -31.6074), (-15.3562, -19.7356), (-48.1437, 9.9446), (-22.7064, 21.2809), (40.1235, -30.6486), (31.5804, -27.9023), (-68.5042, -25.7727), (49.0589, 45.1601), respectively, all in meters.

The maximum transmission power of a GAA user is 23 dBm across all RBG [3]. We consider a total of 18 RBGs to be allocated to GAA users. The interference and transmission channel gains associated with these RBGs are modeled based on path loss and Rayleigh fading. The path loss model for GAA users follows the same ITU indoor path loss model. We calculate the gain of the transmission channel as follows:  $h_{iB}^g = PL_{\text{GAA}}(d_{iB}) \cdot f_{iB}^g,$  where  $f_{iB}^g$  represents the fast fading between the *i*-th GAA user and its CBSD in RBG g, and  $d_{iB}$ represents the distance between the GAA user i and its BS. Thermal noise on each RBG in the GAA BS is  $8 \times 10^{-7}$  mW. Similarly, the interference channel gain between the i-th GAA user and the j-th PAL user can be calculated as follows:  $h_{ij}^g =$  $PL_{GAA}(d_{ij}) \cdot f_{ij}^g$ , where  $f_{ij}^g$  represents the fast fading between the GAA user i and its nearby PAL user j on RBG g, and  $d_{ij}$ is the distance between i-th GAA user and j-th PAL user.

Note that our proposed Mitra does not assume any knowledge of channel distributions. But in our simulation study, we must use some distributions to generate the random channel gains. There is no conflict here, as such distribution information is purposely withheld from Mitra.

We compare Mitra with two benchmarks:

- Mean formulation: We use the mean of the interference channel gain  $(\mathbf{h}_j)$  as the perfect CSI, which transforms our initial chance constraint (7) into a deterministic counterpart with constant interference channel gain. We can then solve this problem easily using an existing optimizer. We used CVX version 2.2 with Gurobi (version 9.11) as the solver in MATLAB.
- Worst-case formulation: We choose the maximum interference channel gain from the available K data samples to represent the worst case. This worst-case assumption will remove uncertainty and convert our CCP into a linear deterministic constraint. We can then solve the reformulated problem easily using the Gurobi solver.

		$ heta_j$						
$\epsilon$	$\rho$	j = 1	j = 2	j = 3	j = 4	j = 5		
0.01	11.2520	0.2068	0.3225	0.3889	0.2254	0.2243		
0.05	7.5023	0.1377	0.2178	0.2619	0.1509	0.1504		
0.10	5.6275	0.1015	0.1620	0.1943	0.1116	0.1107		

TABLE II ACTUAL VIOLATION PROBABILITY  $\epsilon_i^*$  OF EACH PAL USER.

		$\epsilon_j^*$						
Algorithm	$\epsilon$	j = 1	j = 2	j = 3	j = 4	j = 5		
Mitra	0.01	0	0	0.0024	0.0097	0.0098		
	0.05	0.0008	0.0009	0.0145	0.0383	0.0414		
	0.10	0.0039	0.0040	0.0415	0.0947	0.0985		
Mean form	-	0.0805	0.0814	0.3240	0.4696	0.4901		
Worst-case	-	0	0	0	0	0		

#### B. Results

We first calculate the  $\theta_j$  values in the non-RT control loop of Mitra. Table I shows the  $\rho$  and  $\theta_j$  values for each PAL user under different  $\epsilon$ 's for the network topology in Fig. 4. From Table I, we see that when  $\epsilon$  increases, the values of  $\theta_j$ 's in any of the five columns decrease. This is intuitive, as the greater the tolerance of interference violation (i.e., the greater the  $\epsilon$  is), the smaller the radius of the Wasserstein ball (search space).

In Mitra's RT control loop, we set L to 2, which results in a total of  $2^{18}$  subproblems. We select 512 subproblems (i.e., S=512) in the reduced search space. We evaluate Mitra for three practical risk levels ( $\epsilon$ ): 0.01, 0.05, and 0.1.

We find that the value of K directly impacts the performance of Mitra, with a larger K generating better objective values. However, the computation time of Mitra increases with respect to K, creating a trade-off between the achieved objective value and K. In [27], we show that it is sufficient to choose K=32 for our problem.

We run Mitra for 50 TTIs (not including the initial window of 5 TTIs). Each run employs K=32 data samples collected from the past 4 TTIs. To evaluate Mitra's solution for each TTI, we generate 1,000 channel instances for each solution and calculate the actual violation probability for each PAL user. Final results are averaged over 50 TTIs.

Table II shows the actual probability of violation  $\epsilon_j^*$  for each PAL user j. Clearly, for each target risk level  $\epsilon$ , the actual probability of violation  $\epsilon_j^*$  for each PAL user remains below the threshold, indicating the efficacy of Mitra. On the other hand, there is a wide variance in the probabilities of violation between PAL users in the mean formulation, with the highest being 49% (for PAL 5). Under the worst-case formulation, the probability of violation for all PAL users is 0, confirming its extreme conservative nature. In Fig. 5(a), we present the averaged  $\epsilon_j^*$  over all PAL from Table II. We see that the averaged  $\epsilon_j^*$  by Mitra is below  $\epsilon$  in all three settings. On the contrary, the average probabilities of violation by the mean formulation are well beyond the target  $\epsilon$ .

Figure 5(b) presents the achieved objective values under different algorithms in this case study. We find that Mitra's performance is at least 85% better than the worst-case formulation and is upper bound by the mean formulation. Furthermore, Mitra's objective value monotonically increases with  $\epsilon$ . This is intuitive, as the higher the probability of violation ( $\epsilon$ ) that the PALs can tolerate, the higher the throughput that GAA users are able to achieve.

To evaluate the timing performance of Mitra's RT control loop, we plot its running time over 50 TTIs under three different risk levels, as shown in Fig. 5(c). As we can see in the figure, Mitra's RT-control loop can meet the 1 ms timing requirement in each TTI for all  $\epsilon$  settings. Further, we find that the running time of Mitra is independent of the  $\epsilon$  value. As a comparison, we also measure the running time of solving OPT-R directly on a solver. The average running time over 50 TTIs is around  $1.2 \times 10^3$  seconds for  $\epsilon = 0.10$ .

## VI. CONCLUSION

The goal of this paper is to design a real-time solution for the coexistence of GAA users with PAL users in the same spectrum in CBRS. To address the lack of cooperation from PAL users and the inherent uncertainty in sensing information, we proposed using limited data samples to infer interference channel information. The objective is to maximize spectrum efficiency using the PF metric for GAA users while providing the necessary interference protection for PAL users. The first novelty of our proposed solution (Mitra) is the use of the ∞-Wasserstein ambiguity set to approximate the unknown distribution of the interference channel gain between GAA and PAL users based on limited data samples through passive sensing. The second novelty of Mitra is its clever exploitation of the non-RT and RT control loops in O-RAN architecture, which allows the solution to be developed in two components across different time scales. The third novelty of Mitra is its innovative use of GPU parallel computing in its design of the RT control loop. Experimental results show that Mitra can achieve coexistence with competitive spectrum efficiency while providing probabilistic interference guarantee to PAL users. It can also meet the 5G RT scheduling requirement (1 ms) in a practical scenario.

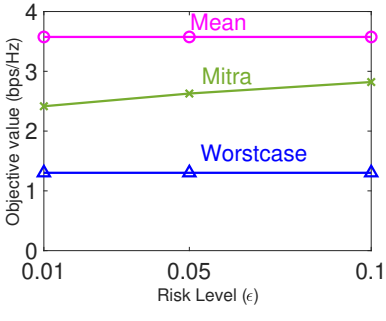
#### ACKNOWLEDGMENTS

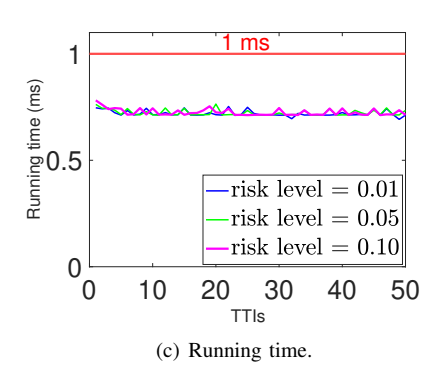
This research was supported in part by ONR under MURI Grant N00014-19-1-2621, NSF under grants 2246414 and 2246417, Virginia Commonwealth Cyber Initiative (CCI), and Virginia Tech Institute for Critical Technology and Applied Science (ICTAS).

# REFERENCES

- [1] The Office of the Federal Register (OFR) and the Government Publishing Office, "OFR: Electronic Code of Federal Regulations, Title 47: Telecommunication, Part 96 Citizens Broadband Radio Service," Available: https://www.ecfr.gov/current/title-47/chapter-I/subchapter-D/part-96 (Last accessed: Feb. 03, 2023).
- [2] M. Woodley, "Using CBRS and haven't heard about TARDYs3? Don't be late to the party," Available: https://www.ericsson.com/en/blog/6/ 2023/impact-of-tardys3-on-cbrs-commercial-operations (Last accessed: July 03, 2023).







(a) Average actual violation probability of PAL users.

(b) Achieved objective value.

Fig. 5. Performance of Mitra under different risk levels.

- [3] Wireless Innovation Forum, "CBRS Deployment Guidelines for Installers, Version V1.2.0," Available: https://winnf.memberclicks.net/assets/CBRS/WINNFTR-5001.pdf (Last accessed: Feb. 08, 2023).
- [4] N. Jai, S. Li, C. Li, Y.T. Hou, W. Lou, J.H. Reed, and S. Kompella, "Optimal Channel Allocation in the CBRS Band with Shipborne Radar Incumbents," in *Proc. IEEE DySPAN*, pp. 80–88, virtual conference, Dec. 13–15, 2021.
- [5] K.S. Manosha, S. Joshi, T. Hänninen, M. Jokinen, P. Pirinen, H. Posti, K. Horneman, S. Yrjölä, and M. Latva-aho, "A Channel Allocation Algorithm for Citizens Broadband Radio Service/Spectrum Access System," in *Proc. Euro. Conf. on Networks and Commun. (EuCNC)*, pp. 1–6, Oulu, Finland, June 12–15, 2017.
- [6] M. Tonnemacher, C. Tarver, V. Chandrasekhar, H. Chen, P. Huang, B.L. Ng, J.C. Zhang, J.R. Cavallaro, and J. Camp, "Opportunistic Channel Access Using Reinforcement Learning in Tiered CBRS Networks," in *Proc. IEEE DySPAN*, pp. 1–10, Seoul, South Korea, Oct. 22–25, 2018.
- [7] R. Karaki and A. Mukherjee, "Coexistence of Contention-Based General Authorized Access Networks in 3.5 GHz CBRS Band," in *Proc. IEEE* 87th Veh. Technol. Conf. (VTC Spring), pp. 1–6, Porto, Portugal, June 3–6, 2018.
- [8] N. Y. Soltani, S.-J. Kim, and G.B. Giannakis, "Chance-Constrained Optimization of OFDMA Cognitive Radio Uplinks," *IEEE Trans. Wireless Commun.*, vol. 12, no. 3, pp. 1098–1107, Mar. 2013.
- [9] L. Wang, M. Sheng, Y. Zhang, X. Wang, and C. Xu, "Robust Energy Efficiency Maximization in Cognitive Radio Networks: The Worst-Case Optimization Approach," *IEEE Trans. Commun.*, vol. 63, no. 1, pp. 51– 65, Jan. 2015.
- [10] M.H. Al-Ali and K.C. Ho, "Transmit Precoding in Underlay MIMO Cognitive Radio With Unavailable or Imperfect Knowledge of Primary Interference Channel," *IEEE Trans. Wireless Commun.*, vol. 15, no. 8, pp. 5143–5155, Aug. 2016.
- [11] Y. Xu, Y. Liu, G. Li, H. Yu, and R. Lai, "Robust Uplink Power Allocation for Two-Tier Heterogeneous Networks," in *Proc. 9th Int'l Conf. on Wireless Commun. and Signal Processing (WCSP)*, pp. 1–5, Nanjing, China, Oct. 11–13, 2017.
- [12] E. Dall'Anese, S.-J. Kim, G.B. Giannakis, and S. Pupolin, "Power Control for Cognitive Radio Networks Under Channel Uncertainty," *IEEE Trans. Wireless Commun.*, vol. 10, no. 10, pp. 3541–3551, Oct. 2011.
- [13] H.A. Suraweera, P.J. Smith, and M. Shafi, "Capacity Limits and Performance Analysis of Cognitive Radio With Imperfect Channel Knowledge," *IEEE Trans. Veh. Technol.*, vol. 59, no. 4, pp. 1811–1822, May 2010.
- [14] F. Wang, C. Xu, L. Song, and Z. Han, "Energy-Efficient Resource Allocation for Device-to-Device Underlay Communication," *IEEE Trans. Wireless Commun.*, vol. 14, no. 4, pp. 2082–2092, Apr. 2015.
- [15] C. Pan, J. Wang, W. Zhang, B. Du, and M. Chen, "Power Minimization in Multi-Band Multi-Antenna Cognitive Radio Networks," *IEEE Trans. Wireless Commun.*, vol. 13, no. 9, pp. 5056–5069, Sep. 2014.
- [16] M. Lu, B. Zhou, Z. Bu, and Y. Zhao, "A Learning Approach Towards Power Control in Full-Duplex Underlay Cognitive Radio Networks," in Proc. IEEE Wireless Commun. and Net. Conf. (WCNC), pp. 2017–2022, Austin, TX, USA, April 10–13, 2022.
- [17] W. Lee, "Resource Allocation for Multi-Channel Underlay Cognitive

- Radio Network Based on Deep Neural Network," *IEEE Commun. Letters*, vol. 22, no. 9, pp. 1942–1945, July 2018.
- [18] W. Lee and K. Lee, "Deep Learning-Aided Distributed Transmit Power Control for Underlay Cognitive Radio Network," *IEEE Trans. on Veh. Technol.*, vol. 70, no. 4, pp. 3990–3994, April 2021.
- [19] 3GPP, 5G; NR; Physical layer procedures for data (3GPP TR 38.214, Version 16.8.0, Release 16, Dec. 2021), Available: https://portal.3gpp.org/desktopmodules/Specifications/SpecificationDetails. aspx?specificationId=3216 (Last accessed: July 08, 2022).
- [20] L. Day, "LTE SNIFFER FERRETS OUT CELLULAR COMMU-NICATIONS," May 2023, Available: https://hackaday.com/2023/05/18/ lte-sniffer-ferrets-out-cellular-communications/ (Last accessed: July 06, 2023)
- [21] N. Jiang and W. Xie, "ALSO-X and ALSO-X+: Better convex approximations for chance constrained programs," *Operations Research*, vol. 70, no. 6, pp. 3581–3600, Feb. 2022.
- [22] Y.T. Hou, Y. Shi, and H.D. Sherali, Applied Optimization Methods for Wireless Networks, ch. 5. Cambridge, U.K.: Cambridge Univ. Press, 2014
- [23] 3GPP, 5G; NR; Physical channels and modulation (3GPP TR 38.211, Version 16.8.0, Release 16, Dec. 2021), Available: https: //portal.3gpp.org/desktopmodules/Specifications/SpecificationDetails. aspx?specificationId=3213 (Last accessed: July 12, 2022).
- [24] O-RAN Alliance (O-RAN Working Group 1), O-RAN Architecture Description, Version O-RAN.WG1.OAD-R003-v08.00, Available: https://orandownloadsweb.azurewebsites.net/specifications (Last accessed: March 05, 2023).
- [25] Nvidia Corp. CUDA Toolkit. Available: https://developer.nvidia.com/ CUDA-toolkit (Last accessed: Dec. 10, 2022).
- [26] 3GPP, LTE; Evolved Universal Terrestrial Radio Access (E-UTRA); Radio Frequency (RF) requirements for LTE Pico Node B (3GPP TR 36.931, Version 16.0.0, Release 16, July 2020), Available: https://portal.3gpp.org/desktopmodules/Specifications/SpecificationDetails.aspx?specificationId=2589 (Last accessed: Mar. 08, 2023).
- [27] S. Acharya, S. Li, N. Jiang, Y. Wu, Y.T. Hou, W. Lou, and W. Xie, "Mitra: An O-RAN based Real-Time Solution for Coexistence between General and Priority Users in CBRS," Available: https://www.cnsr.ictas. vt.edu/publication/shiva\_2023.pdf (Last accessed: July 11, 2023).